Astron. Astrophys. 333, L51–L54 (1998)

ASTRONOMY AND ASTROPHYSICS

LETTER

Letter to the Editor

76 mas speckle-masking interferometry of IRC +10 216 with the SAO 6 m telescope: Evidence for a clumpy shell structure

G. Weigelt[1], **Y. Balega**[2], **T. Blöcker**[1], **A.J. Fleischer**[3], **R. Osterbart**[1], **and J.M. Winters**[3]

[1] Max-Planck-Institut für Radioastronomie, Auf dem Hügel 69, D-53121 Bonn, Germany
[2] Special Astrophysical Observatory, Nizhnij Arkhyz, Zelenchuk region, 35147 Karachai-Cherkesia, Russia
[3] Technische Universität Berlin, Institut für Astronomie und Astrophysik, Sekr. PN 8-1, Hardenbergstrasse 36, D-10623 Berlin, Germany

Received 18 December 1997 / Accepted 10 March 1998

Abstract. We present the first K′-band image of the carbon star IRC +10 216 with 76 mas resolution. The diffraction-limited image was reconstructed from 6 m telescope speckle data using the speckle masking bispectrum method. The image shows that the dust shell of IRC +10 216 is extremely clumpy. Five individual clouds within a $0\farcs21$ radius of the central star have been resolved for the first time. On the basis of consistent theoretical models we argue that these structures are produced by circumstellar dust formation. The fragmentation of the shell structure gives most likely direct evidence for an inhomogeneous mass-loss process which may be interpreted in terms of large-scale surface convection-cells (Schwarzschild 1975) being a common phenomenon for red giants.

Key words: techniques: image processing – stars: carbon – circumstellar matter – stars: individual: IRC +10 216 – stars: mass-loss – stars: AGB, post-AGB

1. Introduction

IRC +10 216 (CW Leo) is the nearest and best–studied carbon star. It is a long–period variable star with a period of about 650 d and a spectral type of C9,5 (see e.g. Olofsson et al. 1982). Estimates of its distance range from 100 pc (Zuckerman et al. 1986) to 290 pc (Herbig & Zappala 1970). IRC +10 216 is surrounded by a dust shell which is expanding at $v_{\rm exp} \approx 15\,{\rm kms}^{-1}$, thereby carrying a mass loss rate of $\dot{M} \approx 2{-}5\,10^{-5} M_{\odot}\ {\rm yr}^{-1}$ (e.g. Loup et al. 1993). The first high-resolution IR observations of the dust shell of IRC +10 216 were reported by Toombs et al. (1972), McCarthy et al. (1980, 1990), Mariotti et al. (1983), Dyck et al. (1984, 1987, 1991), Ridgway & Keady (1988), Christou et al. (1990), Le Bertre et al. (1988), Danchi et al. (1994), Osterbart et al. (1997), and Weigelt et al. (1997). Detailed radiation transfer calculations for IRC +10 216 have been carried out, for instance, by Groenewegen (1997) using a large amount of spectroscopic and visibility data. Consistent time–dependent models describing the circumstellar shells of dust forming long–period variables have been presented by Fleischer et al. (1992). A general result of these models is the formation of discrete dust layers, causing pronounced time–varying, step–like surface intensity distributions (Winters et al. 1995).

In this *Letter* we present diffraction-limited 76 mas speckle masking observations of the clumpy dust shell of IRC +10 216. We speculate about the origin of these structures in the light of consistent time–dependent model calculations and discuss the red giants' large-scale surface convection (Schwarzschild 1975) as a possible mechanism for inhomogeneous mass loss.

2. Observations and speckle masking results

The IRC +10 216 speckle interferograms were obtained with the 6 m telescope at the Special Astrophysical Observatory on April 3, 1996 (variability phase 0.10). The speckle interferograms were recorded with our NICMOS 3 camera through a standard K′ filter with a center wavelength of 2.17 μm and a bandwidth of 0.33 μm. 968 IRC +10 216 speckle interferograms and 1496 reference star interferograms (HIC 51133) were recorded. The observational parameters were as follows: exposure time per frame 70 ms, pixel size 14.6 mas, and seeing (K′) $\sim 2\farcs5$. Fig. 1 shows the diffraction-limited K′ image of IRC +10 216 which was reconstructed from the speckle interferograms using the speckle masking bispectrum method (Weigelt 1977, Lohmann et al. 1983, Weigelt 1991; note that the image published by Weigelt et al. (1997) was actually a K′ image, not an H-band image as was incorrectly printed). In addition to the dominant central object A, three bright knots (called B, C, and D) can be identified. The separation of B, C, and D from the central object are $\sim$ 203 mas, 137 mas, and 136 mas, respectively. The position angles of B, C, and D are 21°, 339°, and 59°, respectively. The reconstructed image shows that the dust shell of IRC +10 216 is extremely clumpy. The asymmetry of the dominant central object suggests that there are at least two additional clouds E and F (not fully resolved) at separations much smaller than the separations of B, C, and D (i.e., at separation < 100 mas). The

Send offprint requests to: G. Weigelt
Correspondence to: weigelt@mpifr-bonn.mpg.de

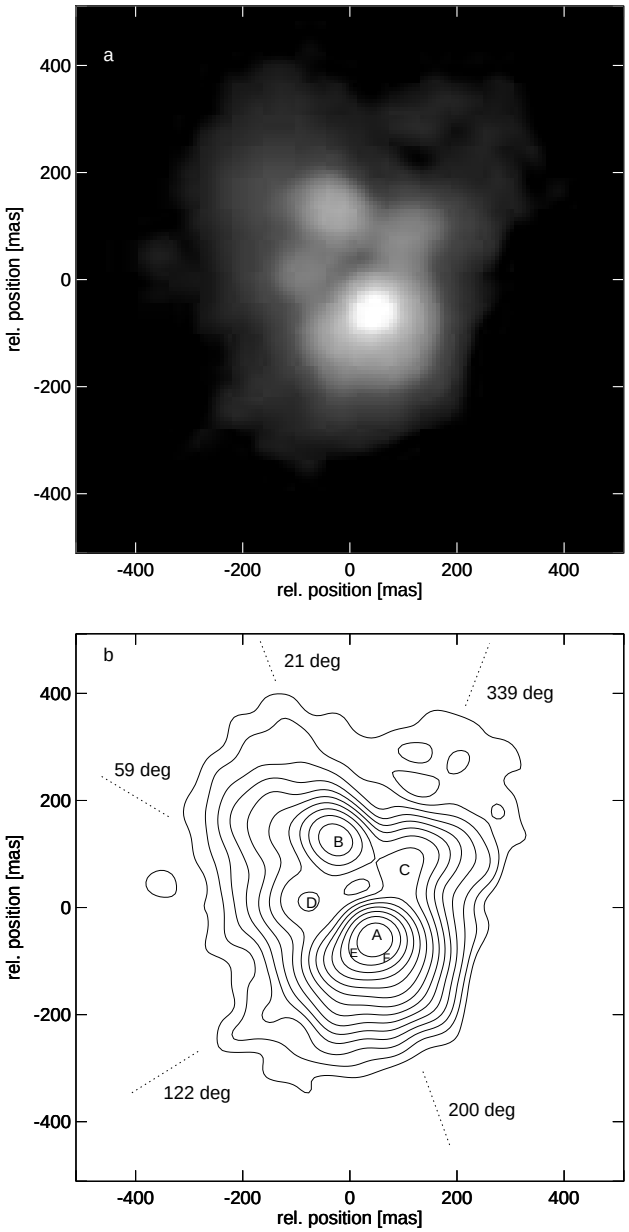

Fig. 1a and b Speckle masking observation of IRC +10 216: **a** K′-band speckle masking reconstruction, **b** contour plot of **a** with the denotation of the components (the contour levels are plotted in steps of 0.3^{m}). The dotted lines indicate the cut directions taken for Figs. 2a–e

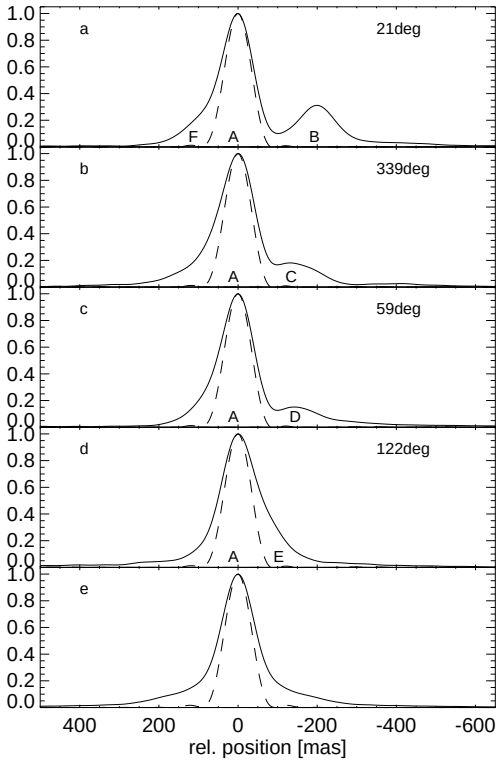

Fig. 2a–e Intensity cuts (solid lines) through the image in Fig. 1 in the indicated directions. The cut directions are shown by dotted lines in Fig. 1b. Dashed curves are cuts through the point spread function reconstructed from two different data sets of the reference star. In plot e the azimuthal averages of IRC +10 216 and the PSF are shown

position angles of E and F are $\sim$ 122° and 200°, respectively. The objects A to F are located inside a larger nebulosity which looks like a bipolar, X–shaped nebula with an approximately NS polar axis (or position angle 10 to 20°, in agreement with Kastner & Weintraub 1994). At the 2% intensity level the nebulosity extends over $0\farcs8$ in NS and $0\farcs6$ in EW direction. The considerable brightness of cloud B ($\sim 5\%$ of the total flux) can, for instance, be explained if we assume that the central star is obscured by a dust disk seen nearly edge-on. The smallest radius of the dominant central object (A+E+F) was measured for position angle 21° (see Fig. 2a). At position angle 21° the radius of the central object was determined to be approximately 25 mas$\pm$8 mas which is an upper limit for the radius of the central star, as the observed central object A could consist of both the stellar disk plus nearby or foreground dust clouds.

3. Discussion

3.1. Evolutionary status

IRC +10 216 is in a very advanced stage of its AGB evolution due to its low effective temperature, long period and high mass-loss rates. Its carbon-rich chemistry indicates that a significant number of thermal pulses with corresponding dredge-up events did take place. The mass of the hydrogen-exhausted core, M_{H}, can be expected to be already close to the later final mass, due to the high mass-loss rates and limited core growth-rates per pulse of only a few $10^{-3} M_{\odot}$ in its stage of evolution (depending on mass) partially compensated or even canceled by dredge-up episodes. The conjecture that IRC +10 216 has entered a phase immediately before moving off the AGB seems to be supported by its non-spherical appearance (Fig. 1; see also Kastner & Weintraub 1994). In contrast to their progenitors, AGB successors often expose prominent features of asphericities, mostly in axisymmetric geometry. Note, that IRC +10 216 is already considerably elongated in NS direction probably even with a *bipolar* structure (Fig. 1).

The measured bolometric flux S at maximum light ($S = 2.1 \cdot 10^{-8}\,\mathrm{W m^{-2}}$; Sopka et al. 1985) leads to $11000 <$

$L/L_\odot < 18900$ for recent distance estimates of $130\,\mathrm{pc} < d < 170\,\mathrm{pc}$ (Le Bertre 1997, Winters et al. 1994a). Introducing these luminosities into the core-mass luminosity relation will give upper limits for M_H since S requires corrections for the mean variability phase and the thermal-pulse cycle phase. Evolutionary models of Blöcker (1995) give $M_\mathrm{H} = 0.65 M_\odot$ for $L = 10000 L_\odot$. Note, that the M_H-L relation breaks down for massive AGB models (Blöcker & Schönberner 1991) due to the penetration of the envelope convection into the hydrogen-burning shell ("hot bottom burning", HBB). Accordingly, the upper luminosity value indicates $M_\mathrm{H} \lesssim 0.8 M_\odot$ and possibly HBB. Since the present core mass will not deviate much from the final mass, it can be applied in initial-final mass relations. Taking the AGB calculations of Blöcker (1995) and Vassiliadis & Wood (1993), resp., we finally arrive at initial masses lower than $2.5-3\,M_\odot$ for $d = 130$ pc and $4-4.5\,M_\odot$ for $d = 170$ pc. The chemistry of the circumstellar envelope gives further constraints. Guelin et al. (1995) compared the observed isotopic abundance ratios with evolutionary models. Particularly the C, N and O isotopic ratios led to the conclusion that the initial mass ranges between 3 and $5 M_\odot$, and that moderate HBB has taken place, favouring an initial mass close to $4\,M_\odot$.

3.2. Discrete dust layers

As a demonstrative example Fig. 3 shows a one–dimensional synthetic intensity profile resulting from a consistent time–dependent model calculation for a carbon–rich circumstellar dust shell. These model calculations assume spherical symmetry and include a consistent treatment of time–dependent hydrodynamics, chemistry, dust formation, growth and evaporation and of the radiative transfer problem (Fleischer et al. 1992, Winters et al. 1994b). A general result of the calculations is the formation of discrete dust layers with the characteristic step–like intensity profile shown in Fig. 3 (top). The location and height of the steps vary in time since the dust layers are moving outwards and, thereby, become geometrically diluted (see Winters et al. 1995). In the calculation, these structures are produced by thermal dust emission which, via the dust opacity, depends on wavelength. Note also, that the steps are separated by only a few stellar radii (lower abscissa; the upper abscissa gives the angular extension assuming $d = 170$ pc). The bottom diagram of Fig. 3 shows the intensity profile convolved with the ideal point spread function (PSF) of the 6 m telescope (FWHM diameter 76 mas). At this resolution the step-like structures in the intensity profile disappear completely. Comparing this intensity profile (Fig. 3, bottom) with our measured one (same figure) shows that there is a good agreement, but the wings of the measured profile are slightly higher.

The most striking structures in our image (Fig. 1) are the three knots B, C, and D. Assuming a typical stellar radius of the central source of $R_* = 5{\cdot}10^{13}$cm and $d = 170$ pc (Winters et al. 1994a), the (tangential) separation of the knots from the central peak is $10\,R_*$ (B) and $7\,R_*$ (C,D). In terms of the models, this could be interpreted as knots B, C, and D being connected to an outer dust layer, whereas knots E and F belong to the next layer

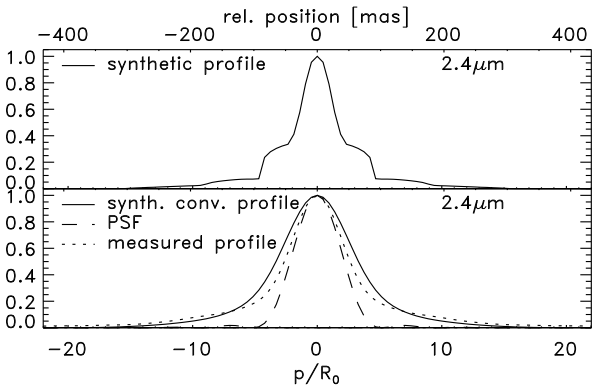

Fig. 3. Synthetic intensity profile at $\lambda = 2.4\mu$m (upper panel) resulting from a model calculation (see text). The lower panel shows the convolution (solid line) of the synthetic profile with the PSF of the 6 m telescope, the PSF of the 6 m telescope (dashed line), and the azimuthal average of the measured intensity (dotted line)

inwards. This interpretation requires the fragmentation of inhomogeneous dust layers or that the knots result from spatially bounded separate dust formation events. Since dust nucleation is extremely sensitive to the local kinetic gas temperature, dust formation could be caused locally even by small temperature fluctuations. The radial velocity of the expanding dust shell is approximately $15\,\mathrm{km\,s^{-1}}$. This corresponds to ~ 3 AU/year or 18 mas/year at a distance of 170 pc for a movement perpendicular to the line–of–sight. Thus, if connected to this expansion, knot B should have formed at least 11.6 yr ago, while C and D would be $\geq$ 7 yr old. In terms of the pulsation period ($P \sim 650$ d) this would correspond to a time scale for the formation of new dust layers (or knots) of $\Delta t \geq 2.5\,P$. Then, the structures E and F would have been formed $\sim 1.5\,P$ ago. The formation of new dust layers on time scales longer than the pulsation period is a common phenomenon of the model calculations (e.g. Fleischer et al. 1992, Winters et al. 1994b, 1995). Therefore, future observations can be used to test this model and to determine the dust formation frequency and the tangential velocity of the structures.

3.3. Inhomogeneuos mass loss

Since the present observations reveal that IRC +10 216's shell structure is *highly fragmented* in the immediate stellar vicinity, there seems to be evidence for an already *inhomogeneous mass-loss process*. Inhomogeneously outflowing matter implies corresponding stellar surface inhomogeneities which may be caused by magnetic activity, global pulsations or large-scale photospheric convection. In particular, the latter seems to be a common phenomenon of far-evolved stars.

Schwarzschild (1975) showed that the typical horizontal size of a solar granule, x_gran, is given by characteristic depth scales of the layers below the photosphere. With the pressure scale height, H_p, as the major depth scale and assuming that the ratio of $x_\mathrm{gran}/H_\mathrm{p}$ is constant he found that for red giants the dominant convective elements become so large that only a few of them can occupy the surface at any time leading to large

temperature variations on the surface and concomitant brightness fluctuations. Due to the prominent temperature contrasts at the surface the emitted radiation is highly anisotropic leading to a polarization of the light scattered by circmstellar dust. Schwarzschild (1975) already supposed that mass ejection is triggered by photospheric convection and Dyck et al. (1987) outlined its possible importance for IRC +10 216.

Indeed, based on a linear stability analysis of convective modes in the envelopes of red giants, Antia et al. (1984) found the pressure scale height to be the prevailing depth scale leading to dominant convective elements which are of comparable size to the stellar radius. More recently, Freytag et al. (1997) presented models for convection zones of main-sequence stars and subgiants with spectral type F to K based on 2D numerical radiation hydrodynamics calculations. They found a tight correlation between the characteristic photospheric scale height $H_{\rm p0} = R_{\rm gas}T_{\rm eff}/g$ and the size of the granules, $x_{\rm gran}$, viz. $x_{\rm gran} \approx 10H_{\rm p0}$ covering more than two orders of magnitudes in gravity. Due to this robustness a (cautious) extrapolation to the red giant regime seems to be justified. For IRC +10 216 (with $T_{\rm eff} = 2200$ K, $R = 700R_{\odot}$, and $M = 0.8M_{\odot}$) this leads to a typical granule size of $x_{\rm gran} \approx 0.82R_{*}$ allowing the whole surface to be occupied by, at most, a few granules.

The resulting temperature fluctuations can be expected to be in the range of up to several hundred Kelvin (Antia et al. 1984) being large enough to cause observable brightness fluctuations and to influence the formation of the shock- and dust-driven stellar wind and, therewith, the shape of the circumstellar shell. Thus, one further implication of large-scale surface inhomogeneities could be a corresponding large-scale fragmentation of the outflowing matter possibly leading to knots within the multiple shell structure as observed for IRC +10 216.

4. Conclusion

Our speckle masking reconstruction of IRC +10 216 shows that the circumstellar dust shell of IRC +10 216 consists of at least five individual dust clouds B to F within a $0\farcs21$ radius of the central star. With $d = 170$ pc and $R_{*} = 5 \cdot 10^{13}$cm, the tangential separations of the clouds B, C, and D from the central star correspond to ~ 34 AU $\sim 10\,R_{*}$ (B) and 23 AU $\sim 7\,R_{*}$ (C,D). Time-dependent calculations for circumstellar envelopes show the formation of multiple-shell structures, and the synthetic intensity profiles agree well with the measured ones. The prominent clumpiness of these very inner shells gives evidence for an already inhomogeneous mass loss which may be intimately linked with large-scale surface inhomogeneities possibly induced by giant surface convection-cells.

Acknowledgements. We thank B. Freytag for valuable discussions on surface convection zones. J.M.W. and A.J.F. thank the Konrad–Zuse–Zentrum für Informationstechnik Berlin and the HLRZ, Jülich for a generous grant of computing time. A.J.F. was supported by the DFG (grant Se 420/8–1) and J.M.W. by the BMBF (grant 05 3BT13A 6).

References

Antia H.M., Chitre M., Narasimha D., 1984, ApJ 282, 574
Blöcker T., 1995, A&A 297, 727
Blöcker T., Schönberner D.. 1991, A&A 244. L43
Christou J.C., Ridgway S.T., Buscher D.F., Haniff C.A., McCarthy jr. D.W., 1990, Astrophysics with infrared arrays, Elston R. (ed.), ASP conf. series Vol. 14, p. 133
Danchi W.C., Bester M., Degiacomi C.G., Greenhill L.J., Townes C.H., 1994, AJ 107, 1469
Dyck H.M., Benson J.A., Howell R.R., Joyce R.R., Leinert C., 1991, AJ 102, 200
Dyck H.M., Howell R.R., Zuckerman B., Beckwith S., 1987, PASP 99, 99
Dyck H.M., Zuckerman B., Leinert C., Beckwith S., 1984, ApJ 287, 801
Fleischer A.J., Gauger A., Sedlmayr E., 1992, A&A 266, 321
Freytag B., Holweger H., Steffen M., Ludwig H.G.,1997, Science with the VLT Interferometer, F. Paresce (ed.), Springer, Berlin, p.316
Groenewegen M.A.T., 1997, A&A 317, 503
Guelin M., Forestini M., Valiron P., Ziurys L.M., Anderson M.A., Cernicharo J., Kahane C., 1995, A&A 297, 183
Herbig G.H., Zappala R.R., 1970, ApJ 162, L15
Kastner J.H., Weintraub D.A., 1994, ApJ 434, 719
Le Bertre T., 1997, A&A 324, 1059
Le Bertre T., Magain P., Remy M., 1988, Messenger 55, 25
Lohmann A.W., Weigelt G., Wirnitzer B., 1983, Appl. Opt. 22, 4028
Loup C., Forveille T., Omont A., Paul J.F., 1993, A&AS 99, 291
Mariotti J.M., Chelli A., Sibille F., Foy R., Lena P., Tchountonov G., 1983, A&A 120, 237
McCarthy D.W., Howell R., Low F.J., 1980, ApJ 235, L27
McCarthy D.W., McLeod B.A., Barlow D., 1990, Astrophysics with infrared arrays, Elston, R. (ed.), ASP conf. series Vol. 14, p. 139
Olofsson H., Johansson L.E.B., Hjalmarsson Å., Nguyen-Quang-Rieu, 1982, A&A 107, 128
Osterbart R., Balega Y.Y., Weigelt G., Langer N., 1997, Planetary Nebulae, Habing H.J., Lamers H.J.G.L.M. (eds.), Kluwer, in press
Ridgway S.T., Keady J.J., 1988, ApJ 326, 843
Schwarzschild M., 1975, ApJ 195, 137
Sopka R.J., Hildbrand R., Jaffe D.T., Gatley I., Roellig T., Werner M., Jura M., Zuckermann B., 1985, ApJ 294, 242
Toombs R.I., Becklin E.E., Frogel J.A., Law S.K., Porter F.C., Westphal J.A., 1972, ApJ 173, L71
Vassiliadis E., Wood P.R., 1993, ApJ 413, 641
Weigelt G., 1977, Optics Commun. 21, 55
Weigelt G., 1991, Progress in Optics Vol. 29, Wolf, E. (ed.), North Holland, Amsterdam, p. 293
Weigelt G., Balega Y.Y., Hofmann K.-H., Langer N., Osterbart R., 1997, Science with the VLT Interferometer, F. Paresce (ed.), Springer, Berlin, p. 206
Winters J.M., Dominik C., Sedlmayr E., 1994a, A&A 288, 255
Winters J.M., Fleischer A.J., Gauger A., Sedlmayr E., 1994b, A&A 290, 623
Winters J.M., Fleischer A.J., Gauger A., Sedlmayr E., 1995, A&A 302, 483
Zuckerman B., Dyck H.M., Claussen M.J., 1986, ApJ 304, 401